HHS Public Access

Author manuscript

Basic Res Cardiol. Author manuscript; available in PMC 2021 January 14.

Published in final edited form as:

Basic Res Cardiol. ; 115(2): 16. doi:10.1007/s00395-019-0772-8.

Selective intrarenal delivery of mesenchymal stem cell-derived extracellular vesicles attenuates myocardial injury in experimental metabolic renovascular disease

Lei Zhang[1,2], **Xiang-Yang Zhu**[1,*], **Yu Zhao**[1,3], **Alfonso Eirin**[1], **Lei Liu**[1,3], **Christopher M. Ferguson**[1], **Hui Tang**[1], **Amir Lerman**[4], **Lilach O. Lerman**[1,4,*]

[1]Division of Nephrology and Hypertension, Mayo Clinic, Rochester, MN 55905, United States

[2]Department of Urology, Zhongda Hospital, Southeast University, Nanjing, 210009, PR China

[3]Department of Internal Medicine, School of Medicine, Southeast University, Nanjing, 210009, PR China

[4]Division of Cardiovascular Diseases, Mayo Clinic, Rochester, MN 55905, United States

Abstract

Background: Extracellular vesicles (EVs) deliver genes and proteins to recipient cells, and mediate paracrine actions of their parent cells. Intrarenal delivery of mesenchymal stem cell (MSC)-derived EVs preserves stenotic-kidney function and reduces release of pro-inflammatory cytokines in a swine model of coexisting metabolic syndrome (MetS) and renal artery stenosis (RAS). We hypothesized that this approach is also capable of blunting cardiac injury and dysfunction.

Methods: Five groups of pigs were studied after 16 weeks of diet-induced MetS and RAS (MetS +RAS), MetS and MetS+RAS treated 4 weeks earlier with a single intra-renal delivery of EVs-rich fraction harvested from autologous adipose tissue-derived MSCs, and Lean and MetS Shams. Cardiac structure, function, and myocardial oxygenation were assessed in-vivo using imaging, and cardiac inflammation, senescence, and fibrosis ex-vivo. Inflammatory cytokine levels were measured in circulating and renal vein blood.

Results: Intrarenal EV delivery improved stenotic-kidney glomerular filtration rate and renal blood flow, and decreased renal release of monocyte-chemoattractant protein-1 and interleukin-6. Furthermore, despite unchanged systemic hemodynamics, intrarenal EV delivery in MetS+RAS normalized cardiac diastolic function, attenuated left ventricular remodeling, cellular senescence and inflammation, and improved myocardial oxygenation and capillary density in MetS+RAS.

Conclusions: Intrarenal delivery of MSC-derived EVs blunts myocardial injury in experimental MetS+RAS, possibly related to improvement in renal function and systemic inflammatory profile. These observations underscore the central role of inflammation in the crosstalk between the kidney and heart, and the important contribution of renal function to cardiac structural and functional integrity in coexisting MetS and RAS.

*Correspondence: Xiang-Yang Zhu, zhu.xiangyang@mayo.edu or Lilach O. Lerman, lerman.lilach@mayo.edu.

Keywords

Mesenchymal stem cells; Extracellular vesicles; Metabolic syndrome; Renal artery stenosis; Myocardium

INTRODUCTION

The metabolic syndrome (MetS) comprises a cluster of comorbidities including hypertension, dyslipidemia, impaired glucose metabolism, and central obesity, which contribute to the risk for type-2 diabetes mellitus, cardiovascular diseases, and all-cause mortality [1]. MetS affect about one third of the population in the United States and increases as the population ages [7]. The presence of MetS is associated with poor prognosis after myocardial infarction, more severe post-infarction left ventricular (LV) dysfunction, and progression to heart failure [49, 52]. MetS has also been related to atherosclerotic renal artery stenosis (RAS) and chronic kidney disease (CKD) [25, 48], and their coexistence, in turn, further disrupts cardiac structure and function, ultimately leading to an increase of cardiovascular morbidity and mortality [26].

Revascularization of the renal artery alone fails to fully improve cardiac function, despite improved blood pressure [10]. Among insults responsible for persistent myocardial damage after remission of hypertension are inflammation and oxidative stress, which might mediate the crosstalk between the kidney and heart [26]. Inflammatory and oxidative stress factors released from the kidney into the systemic circulation may accelerate the impairment of cardiac function and structure [9, 11]. Our previous studies also demonstrated that revascularization of the stenotic renal artery could not restore glomerular filtration rate (GFR), and the persistently impaired kidney continued releasing inflammation cytokines [41]. Therefore, effective strategies to improve renal function and reduce production and secretion of noxious factors might be fundamental for preservation of cardiorenal function.

Accumulating evidence has uncovered a distinct potential of mesenchymal stem cells (MSCs) for both renal and cardiac repair [38]. We have shown that intrarenal delivery of autologous adipose tissue–derived MSCs alleviated inflammation and oxidative stress, and improved both renal and cardiac function in swine RAS models [12, 15]. MSCs exert their effects via paracrine activity, which is at least partially mediated by extracellular vesicles (EVs), including exosomes (30–150 nm diameter) and microvesicles (MVs) (100–1000 nm diameter) [2, 30]. MSC-derived EVs mimic the function of parental MSCs by shuttling their functional components, such as DNA, RNA, proteins/peptides, and lipids to recipient cells, thereby reducing tissue injury and/or enhancing repair. Our group recently demonstrated that intrarenal delivery of MSC-derived EVs preserved stenotic-kidney function, and reduced systemic oxidative stress and inflammation in a novel experimental model of coexisting swine MetS and RAS (MetS+RAS). MSC exert paracrine release of soluble immunomodulatory factors as long as they engraft and survive in the kidney tissue. In contrast, EVs are taken by target cells, do not replicate, and their effect might thus be short-lived. Therefore, whether selective intrarenal EV delivery is capable of blunting cardiac injury and dysfunction is unclear [16].

Notably, in the microenvironment of MetS+RAS, abnormal glucose metabolism, lipodystrophy, oxidative stress, chronic inflammation might induce cellular senescence [28]. Senescent cells can originate from most cell types and entail essentially irreversible replicative arrest, and apoptosis resistance. Senescent cells frequently exhibit a pro-inflammatory, injurious senescence-associated secretory phenotype (SASP) [34]. Previous studies revealed that cardiac senescence may occur in cardiomyocytes [46], and is involved in pathological cardiac remodeling. However, whether cardiac senescence occurs in the MetS+RAS models and whether it is affected by improving renal function using intra-renal MSC-derived EVs remains unknown.

Therefore, using a swine model of MetS+RAS, we tested the hypothesis that MSC-derived EVs would ameliorate cardiac dysfunction and senescence in MetS+RAS by improving stenotic-kidney function and attenuating circulatory inflammation cytokines.

MATERIALS AND METHODS

Twenty-four domestic female pigs (Manthei Hog Farm, Elk River, MN) were studied during 16 weeks of observation. Animal studies have been approved by the Mayo Clinic Institutional Animal Care and Use Committee and have therefore been performed in accordance with the ethical standards laid down in the 1964 Declaration of Helsinki and its later amendments. At baseline, 22 pigs started a high-cholesterol/high-fructose diet (MetS) for the entire course of the study, whereas the other six were fed regular pig chow (Lean) [37] (Figure 1A).

Six weeks later, pigs were anesthetized with 0.25g of IM tiletamine hydrochloride/zolazepam hydrochloride (Telazol®, Zoetis, Kalamazoo, MI) and 0.5g xylazine (Xylamed, VetOne, Bimeda-MTC Animal Health, Cambridge, ON, Canada), and maintained with IV ketamine (0.2 mg/kg/min, Ketaset, Zoetis, Kalamazoo, MI) and xylazine (0.03 mg/kg/min). Unilateral RAS was induced in 12 MetS pigs by placing an irritant coil in the main renal artery under fluoroscopic guidance (Siemens, Munich, Germany) [31]. This procedure produces a gradual narrowing of the renal artery and increases blood pressure within 3–7 days [12, 15]. Lean and the other MetS pigs underwent a sham procedure. Blood pressure was continuously recorded by an implantable telemetry system (Data Sciences International, St. Paul, MN) [55]. In all animals, abdominal adipose tissue was collected through a biopsy 3 weeks later, and subsequently used to harvest autologous MSCs and isolate their EVs.

Six weeks after induction of RAS or sham, the degree of stenosis was determined using renal angiography. Six MetS+RAS and 4 Mets pigs then received a single infusion of an EV-rich fraction (approximately 10^11 autologous EVs harvested from the culture media of 10x10^6 adipose tissue-derived MSC, a dose used for delivery) into the stenotic kidney over 5 min through a 5-F catheter positioned proximal to the stenosis. Three other groups of Lean, MetS, and MetS+RAS pigs (n=6 each) received PBS vehicle infusion to serve as controls (Figure 1A). Four weeks later, pigs were anesthetized and renal angiography repeated. Mean arterial pressure was measured using a catheter through carotid artery. Single-kidney GFR, renal blood flow (RBF), and cardiac function were assessed using multi-detector computed tomography (MDCT, Somatom Sensation-128, Siemens), and

myocardial oxygenation by blood oxygen level-dependent magnetic resonance imaging (BOLD-MRI). Renal vein (RV) and inferior vena cava (IVC) blood samples were also collected for inflammatory cytokine levels.

Pigs were euthanized with an intravenous bolus of 100 mg/kg of sodium pentobarbital (Fatal Plus, Vortech Pharmaceuticals, Dearborn, MI) 3 days later. Kidneys and heart were dissected, and sections frozen in liquid nitrogen or preserved in formalin for histology and *ex-vivo* studies.

Renal Function

Stenotic-kidney RBF and GFR were measured using MDCT as previously described [8]. Briefly, 140 consecutive scans (330ms each) were performed following a central venous injection of iohexol (350 mg/ml per 2 seconds, GE Healthcare, Marlborough, MA), and images reconstructed and displayed with the Analyze™ software package (Biomedical Imaging Resource, Mayo Clinic, Rochester, MN). Data were analyzed by selecting renal cortex and medulla regions of interest from cross-sectional images, which generates tissue attenuation curves. RBF was calculated by summing the products of cortical and medullary perfusions and corresponding volumes, whereas GFR was assessed from the cortical curve using the slope of the proximal tubular curve [9, 11].

Cardiac function and oxygenation

For cardiac systolic and diastolic functions and LV muscle mass (LVMM), the entire heart was scanned 20 times using MDCT throughout the cardiac cycle, as described [55]. Images were analyzed with Analyze™. Early (E) and late (A) LV filling rate were obtained from the positive slopes of volume/time curves and E/A ratio calculated using MATLAB 7.10 (Math-Works, Natick, MA) [32]. Myocardial perfusion was calculated from time-attenuation curves obtained from the anterior cardiac wall at baseline and after a five-minute intravenous infusion of adenosine (400 μg/kg/min, Sigma-Aldrich, St. Louis, MO) [12].

BOLD-MRI studies were performed on a 3T, Signa EchoSpeed (GE Medical Systems, Milwaukee, WI) scanner, as described [13]. Briefly, animals were anesthetized with 1-2% isoflurane and scans performed during suspended respiration. The relaxivity index R2*, which is inversely related to tissue oxygenation, was calculated in each voxel by fitting the MR signal intensity versus echo times to a single exponential function. For data analysis, regions of interest were traced in the septum in each slice and the images analyzed using MATLAB 7.10.

MSC and EV harvesting

Abdominal subcutaneous adipose tissue (5-10g) was collected from pigs 3 weeks after induction of RAS or sham, processed for MSC isolation using collagenase type-I with a standard protocol, and cultured with advanced MEM medium (Gibco) supplemented with 5% platelet lysate in 37°C/5% CO_2[12]. MSCs were kept in cell recovery medium, and then characterized by the expression of common MSC markers (CD44, CD90, and CD105), and negative expression of CD45, CD34, CD14 surface molecules, using immunofluorescent

staining and flow cytometry, and their trans-differentiation into adipocytes, chondrocytes, and osteocytes [13, 57].

For comparability and uniformity, our EV dose selection was based on the same MSC dose used in our previous studies[12, 56]; we therefore collected EVs released from 10^7 MSC, typically yielding approximately 10^{11} EVs. EV-rich fractions were obtained from supernatants of 10^7 MSCs, cultured in MEM medium without supplements for 48h (to increase EV release), and ultracentrifuged twice [14, 16]. Briefly, after centrifugation at 2000g for 20 min, supernatants were ultracentrifuged at 100,000g (Beckman Coulter Optima L-90 K) for 1h at 4°C, then washed in serum-free medium-199 containing HEPES 25mM, and underwent a final ultracentrifugation. Pellets were suspended, and protein content quantified. Endotoxin contamination was excluded by Limulus testing (Charles River Lab), and EV-rich fractions stored at −80°C until delivery. This EV isolation method has been one of the most widely used, especial with limitations in albumin impurity[3, 42].

Transmission electron microscopy (JEOL 1200 EXII) was used to investigate the size and structure of MSC-derived EV-rich fractions. The MSC supernatant was stained with 2% uranyl acetate (negative staining), and cup-shaped 40–1000nm structures were identified as EVs. Concentration and size distribution of isolated EV-rich fractions was assessed by nanoparticle tracking analysis (NanoSight, Salisbury, UK). EV-rich fractions from MSCs were then characterized based on the expression of the EV (CD9, CD81) and MSC (MHC-class I and CD44) markers by flow cytometry [14].

EV tracking and tissue distribution

EV-rich fractions were labeled prior to delivery with the red fluorescence dye PKH26 (Sigma-Aldrich, St. Louis, MO) according to instructions. Briefly, EV-rich fractions were incubated in 2×10^{-6} M PKH26 (in 2ml) for 5min, and 2ml culture-media with 10% EV-depleted FBS added to stop the reaction. EV-rich fractions were then centrifuged 1h at 100,000g to remove excess dye and resuspended in 5ml DPBS for injection. Labeled EV clusters were subsequently tracked and counted in about 10-15 high-magnification fields in each slide randomly and averaged, in 5μm frozen sections from the heart and stenotic kidney [16].

Myocardial remodeling and fibrosis

LV cross-sections (5μm) were stained with Wheat Germ Agglutinin (WGA, Cat#W11262, Thermo Fisher, Waltham, MA) to assess cardiomyocyte cross-sectional area [53] and with trichrome (Cat# 9179; Newcomer Supply, Middleton, WI) to assess fibrosis. Slides (one per animal) were examined and semi-automatically quantified using ZEN® (Carl Zeiss Microscopy, Cambridge, UK) [12]. Hematoxylin & eosin (H&E) staining was performed to assess capillary density [33]. In each slide, 10-15 high-magnification fields were selected randomly and results from all fields were averaged. To assess angiogenic signaling, myocardial expression of vascular endothelial growth factor (VEGF, Santa Cruz, Dallas, Texas, 1:200) was measured by western blot in homogenized LV myocardium.

Senescence and inflammation

Cellular senescence was detected by the expression of $p16^{INK4}$ and senescence-associated beta-galactosidase (SA-ß-gal) activity. For $p16^{INK4}$, 5μm paraffin cardiac sections were stained with a primary anti-$p16^{INK4}$. On 5μm frozen sections SA-ß-gal staining followed manufacturer's protocol (#9860, Cell Signaling Technology, Danvers, MA), and counterstained with eosin.

Levels of inflammatory cytokines were tested in blood samples from the IVC and stenotic-kidney RV. Levels of monocyte-chemoattractant protein (MCP)-1 were measured by ELISA, and tumor necrosis factor (TNF)-a, interleukin (IL)-6, and IL-1ß by Luminex (Millipore, Billerica, MA) [16]. Their net renal release ([RV-IVC]*RBF) was calculated. Inflammation was also evaluated in heart tissue by western blot normalized for GAPDH loading control, to detect MCP-1 (Cat#ab9669, abeam, Cambridge, UK, 1:500), TNF-α (Cat#SC133193, Santa Cruz, 1:200), IL-6 (cat#ab6672, abeam, 1:1000), and IL-1β (cat#80829, Santa Cruz, 1:200).

Statistical methods

Statistical analysis was conducted using JMP 13.0 software package (SAS Institute, Cary, NC). All data are presented as means±SD. Comparisons within and among groups were performed using a paired Student's *t*-test and ANOVA, respectively. Data that did not follow a Gaussian distribution were compared with nonparametric tests (Wilcoxon and Kruskal Wallis). Statistically significant differences were considered when $p< 0.05$.

RESULTS

Systemic characteristics and cardiac function

The systemic characteristics in all pigs 4 weeks after EVs or sham are summarized in Table 1. Body weights were higher in all MetS compared with lean groups. All RAS pigs developed a similar elevated blood pressure and significant degree of RAS. The stroke volume was significantly increased in MetS+RAS+EV compared with lean pigs. Compared with lean and MetS, cardiac output was significantly higher in the MetS+RAS group but decreased after EV treatment. There were no differences among the groups in heart rate, end diastolic volume, end systolic volume, ejection fraction or systemic vascular resistance. RAS increased LVMM and decreased E/A ratio, but both were blunted by EVs delivery. Basal myocardial perfusion did not differ among the groups, whereas its response to adenosine was impaired in the MetS and Mets+RAS groups, but alleviated in Mets+RAS+EVs pigs. EV delivery did not affect cardiac function in MetS. Furthermore, compared with the lean group, progressively elevated myocardial BOLD-R2* values in the MetS and MetS+RAS groups were observed, which reverted to levels not different from normal in MetS+RAS +EVs (Figure 2A).

EV characterization and EV tracking

Isolated and cultured MSC expressed typical markers, and transdifferentiated into adipocytes, chondrocytes and osteocytes, as previously shown [13, 57]. Transmission electron microscopy demonstrated that smaller MSC-derived EV exhibited the typical round ("cup") appearance of lipid bilayer vesicles on negative staining (Figure 1B). NanoSight

analysis indicated particle size distribution of are 30–1000nm (Figure 1C) (including EVs, although some might represent other particles), and flow cytometry confirmed expression of characteristic EV and MSC markers, as we have previously shown [14] (data not shown).

Labeled EV-rich fractions were identified in frozen sections from the heart and stenotic kidneys. We found stenotic kidney EV-rich fractions retention by 4 weeks after injection of about 10 clusters per field, which was almost 3.4-fold higher ($p<0.05$) than in the heart (Figure 1D).

EV-rich fractions restored function and decreased inflammatory cytokine release in the stenotic kidney

Stenotic-kidney RBF and GFR, which were higher in MetS compared with Lean, decreased in MetS+RAS compared to Mets, but did not differ from MetS in MetS+RAS group after EV-rich fractions treatment. Serum creatinine also fell in MetS+RAS+EVs compared with MetS+RAS (Table 1).

RV levels of MCP-1, TNF-a, IL-6, and IL-1β were elevated in MetS+RAS, and decreased in MetS+RAS+EVs (Figure 2B). IVC levels showed a similar pattern, although differences in TNF-α among the groups did not reach statistical significance, and IL-6 levels in MetS +RAS were not significantly elevated (Figure 2C), but EV-rich fractions decreased IVC levels of all cytokines except for TNF-α. Furthermore, net renal release of MCP-1 and IL-6 decreased in EV-rich fractions treated pigs, and that of IL-1β normalized compared to MetS. Net renal release of TNF-α and IL-6 was higher in MetS+RAS compared with Lean and MetS (Figure 2D). Most cytokines in MetS+EVs pigs were not statistically different from Mets, although the levels of IL-6 were no longer elevated compared to normal pigs.

Intrarenal EV-rich fractions delivery ameliorated myocardial remodeling and fibrosis

Myocyte cross-sectional area was higher in MetS+RAS compared with lean and MetS, but improved in EVs-treated pigs (Figure 3A). Myocardial fibrosis was elevated in all MetS groups, and was most severe in MetS+RAS compared with lean, yet was attenuated in EVs-treated pigs (Figure 3B).

As shown in Figure 3C, MetS pigs exhibited fewer capillaries in the LV myocardium, most prominently MetS+RAS. EV-rich fractions treatment ameliorated capillary density relative to MetS+RAS. Consistently, VEGF expression was decreased in both MetS and MetS+RAS groups, but normalized by EV-rich fractions treatment (Figure 3D).

EV-rich fractions intrarenal delivery alleviated myocardial cellular senescence-like phenotype

Cyclin-Dependent Kinase Inhibitor 2A (CDNK2A; $p16^{INK4}$) is a senescence-related gene, and an important effector of senescence [45]. The percentage of $p16^{INK4}$+ cells was remarkably higher in MetS+RAS compared with lean and MetS, but decreased in MetS +RAS+EVs (Figure 4A), although it remained higher than normal. Senescent cells are also characterized by increased enzymatic activities of lysosomal hydrolase SA-ß-gal. SA-ß-gal

activity was up-regulated in MetS and further in MetS+RAS compared to lean and MetS, but was blunted in MetS+RAS+EVs (Figure 4B).

EV-rich fractions intrarenal delivery attenuated myocardial inflammation

Western blot showed elevated myocardial expressions of MCP-1 and TNF-α in MetS and MetS+RAS, and of IL-6 in MetS+RAS group, EV-rich fractions treatment decreased their expressions compared with sham-treated MetS+RAS (Figure 4C). IL-1β expression tended to increase in MetS+RAS, but no significant differences were detected among the groups due to large variability.

DISCUSSION

The present study demonstrates that despite sustained hypertension, a selective injection of MSC-derived EVs into the stenotic kidney can improve myocardial injury in experimental MetS+RAS. MSC-derived EVs ameliorated myocardial fibrosis and remodeling, attenuated myocardial hypoxia, improved capillary density and microvascular function, and alleviated myocardial cellular senescence, in association with improved diastolic function. Attenuated myocardial injury might be related to the capacity of MSC-derived EVs to improve renal function and decrease stenotic kidney release of inflammatory cytokines, such as MCP-1, TNF-α and IL-6. These observations underscore the central role of inflammation in the crosstalk between the kidney and heart, and emphasize the important impact of renal function on cardiac structure and function (Figure 5).

MetS is an emerging risk factor for cardiovascular morbidity and mortality, is linked to renal impairment [48, 49], and correlates with increased peripheral arterial disease secondary to accelerated atherosclerosis [25], most frequently in the coronary, renal and carotid arteries [4]. RAS results in renal dysfunction due to chronic ischemia, and triggers renovascular hypertension, which further induces myocardial injury and diastolic dysfunction [26]. Moreover, MetS is associated with progression to hemodialysis following renal endovascular intervention for atherosclerotic RAS [6]. Traditional therapy options are limited, warranting identification of more effective strategies to preserve renal and cardiac function.

Renal insufficiency is an independent predictor of cardiovascular morbidity and mortality [18], underpinning the high mortality in these patients. Coexistence of renal and cardiac dysfunction significantly aggravates clinical outcomes, whereas renal replacement therapy improves prognosis [51], highlighting the interactions between the kidney and heart. Our previous studies have shown that cardiac function in swine RAS correlated with renal function [50]. While endogenous circulating EV can partly repair cardiac injury [5], they often do not suffice to achieve full repair. Intrarenal delivery of endothelial progenitor cells or MSCs that improved stenotic-kidney function in turn attenuated cardiomyopathy and improved cardiac function [12, 13]. Similarly, stenotic kidney function improved after MSC-EVs treatment [16]. This study extends our previous observations and demonstrates that selective intrarenal MSC-EVs delivery also improves cardiac diastolic function (E/A) in MetS+RAS, although EDV remained unchanged possibly due to the small sample size. Nevertheless, interventions aimed at improving renal function might be useful for cardiac

protection. In support, a recent study demonstrated that in early-stage CKD myocardial fibrosis does not progress if renal function remains stable [21].

Traditionally, cardiorenal interactions have been attributed to intrarenal and systemic hemodynamic factors [39]. However, therapeutic approaches that target hemodynamic forces have been largely unsuccessful [26], suggesting that underlying disturbances are not limited to hemodynamics. Additional mediators implicated in cardiorenal dysfunction included the renin–angiotensin or sympathetic nervous system activities, as well as non-traditional factors, like inflammation, oxidative stress, anemia, arterial stiffness, and uremic toxins [43].

Inflammation is a crucial link for increased cardiovascular risk [27], especially in the setting of kidney disease. Previously, we have shown enhanced inflammatory status in post-stenotic swine and human kidneys, which might contribute to renal injury and dysfunction [9, 11]. Furthermore, inflammatory mediators released into the systemic circulation might damage the remote myocardium [13]. Here, we found MetS magnifies systemic inflammation by release of cytokines (e.g. MCP-1). With concurrent MetS+RAS, the stenotic kidneys release additional pro-inflammation cytokines (e.g. IL-1β, IL-6, TNF-α), so that their circulating levels are further increased and may enhance cardiac inflammation. Therefore, maneuvers that decrease inflammation might preserve renal and cardiac function in these pathological conditions. Endogenous MSC may reside in adipose tissue in vivo in small numbers, but might be overwhelmed in disease conditions, and do not necessarily reach the systemic circulation or remote target organs in sufficient numbers. MSC expansion in vitro enables harvesting large numbers of MSC and EV, and injecting them directly into an organ of interest. We have shown before that intrarenal MSCs delivery reduced inflammation and ameliorated dysfunction in the post-stenotic kidney in swine [13, 57] and human [40]. However, concerns about adverse effects of transplantation of viable replicating cells may limit their translational capacity [19, 29]. MSCs produce a large amount of EVs, which can circumvent some of these concerns [22]. EVs can be internalized into recipient cells and activate signaling by delivering genes and proteins that support extracellular matrix remodeling, inflammation, and angiogenesis [14, 17]. Our recent studies showed the potency of MSC-EVs in restoring hemodynamics and ameliorating renal injury in chronic experimental MetS+RAS [14, 16]. Intrarenal delivery of MSC-EVs decreased renal release pro-inflammatory cytokines, and upregulated IL-10 expression, suggesting that anti-inflammatory properties underpin some of the protective effects of EVs on the stenotic kidney [16]. The current study extends our previous findings, and shows that systemic levels of MCP-1, IL-6 and IL-1β are elevated in MetS+RAS, suggesting a mechanism by which the injured kidney can exert a marked adverse impact on remote organs. Congruently, we also detected upregulated protein expression of MCP-1, TNF-α and IL-6 in the myocardium. Remarkably, EV treatment restored renal function and normalized pro-inflammatory cytokines levels in both the systemic circulation and myocardium. While some EVs were detected in the myocardium, their retention was more than 3-fold lower than in the stenotic-kidney, arguing against a major direct effect of EV on the heart.

Inflammation can directly drive myocardial remodeling [47]. For example, we have shown that MCP-1 mediates myocardium fibrosis, vascular remodeling, and diastolic dysfunction [32]. TNF-α and IL-6 are also associated with LV cardiomyocyte hypertrophy and

dysfunction [23, 54]. In this study, despite sustained hypertension, MetS+RAS-induced cardiomyocyte hypertrophy and fibrosis were attenuated in EV–treated MetS+RAS pigs, likely secondary to amelioration of renal and in turn systemic inflammation. Furthermore, LV myocardial capillary density was reduced in MetS and RAS. MetS+RAS-induced inflammation was also associated with increased hypoxia, which triggers a vicious cycle of progressive cardiac fibrosis and vascular remodeling. Under the persistent metabolic burden of chronic MetS, oxygen demand is magnified but unmet by the capacity to form new vessels. Unlike acute hypoxia, hypoxia in MetS pigs failed to induce VEGF expression, and instead elicited a decrease in vascular density, in line with previous reports [20, 33, 36]. This deleterious situation was aggravated by superimposition of hypertension, but resolved by MSC-EVs treatment. Further studies are needed to define how myocardial angiogenesis is disrupted in MetS and RAS.

Interestingly, we observed cellular senescence-like phenotype in MetS pig myocardium, which might involve cardiomyocytes, interstitial, and endothelial cells. Cardiomyocytes, post-mitotic neurons, and adipocytes show senescence-associated properties, suggesting that post-mitotic cell senescence might be a broad phenomenon, which may not be limited to proliferating cells [24, 35, 46]. The microenvironment of MetS+RAS may induce cellular senescence, which we identified by increased gene expression of CDKI-$p16^{INK4}$ and enhanced SA-ß-gal activity. SA-ß-gal staining in the myocardium is sparse compared with $p16^{INK4}$, possibly because of the variability of basal SA-ß-galactosidase levels [44]. In addition, we cannot exclude the possibility that SA-ß-galactosidase was expressed in infiltrating inflammatory cells, or that elevated myocardial expression of cytokines originated partly from senescence cells SASP that may contribute to inflammation, impaired angiogenesis, and fibrosis during cardiac remodeling (Figure 5).

This study has some limitations, including the short duration of MetS and RAS and use of relatively young pigs, with slower disease progression compared to humans. Nevertheless, our MetS pigs developed obesity, hypertension, hyperlipidemia, and glucose intolerance, which impart subtle changes on structure and function of the heart and kidney [14]. Superimposition of RAS markedly aggravated MetS-induced injury. We cannot exclude direct effect of MSC-EVs towards cardiac improvement, but considering their limited myocardial retention compared to the rather large diminution in levels of circulating pro-inflammatory cytokines, the contribution of EVs was likely small. Some of the observed particles may represent dye transferred from EV to cell membranes. The small sample size and large variability might impede detection of statistically significant differences in the release levels of cytokines. Some tissue studies were not available in the MetS+EV group. Yet, EV did not make a significant impact on *cardiac function or inflammatory cytokines in MetS alone, possibly because of the subtle changes observed in MetS and due to the small sample size.* In addition, we cannot exclude effect of changes in extracellular fluid volume or additional factors linking renal to myocardial function. Further work is needed to identify the types of cardiac cells involved in this crosstalk.

In summary, the present study shows that experimental MetS+RAS induces impairment of the myocardial structure and diastolic function, which might be partly mediated by renal dysfunction and release of pro-inflammation cytokines. Selective intrarenal delivery of

MSC-derived EVs improved renal function and reduced circulating levels of inflammatory cytokines, and thereby ameliorated myocardial remodeling, microcirculation, and senescence, and improved cardiac diastolic function. These salutatory benefits were conferred without any change in systemic hemodynamics. Thus, our study underscores the interactions between the kidney and heart, and implicates circulating mediators induced or released by dysfunctional kidneys in imposing structural and functional impairment in the remote myocardium. It also emphasizes the importance of a healthy kidney to sustain cardiac integrity.

Acknowledgments

SOURCES OF FUNDINGS

This study was partly supported by NIH grant numbers: DK120292, DK104273, HL123160, and DK102325, and DK106427.

REFERENCES

1. Alberti KG, Eckel RH, Grundy SM, Zimmet PZ, Cleeman JI, Donato KA, Fruchart JC, James WP, Loria CM, Smith SC Jr., International Diabetes Federation Task Force on E, Prevention, Hational Heart L, Blood I, American Heart A, World Heart F, International Atherosclerosis S, International Association for the Study of O (2009) Harmonizing the metabolic syndrome: a joint interim statement of the International Diabetes Federation Task Force on Epidemiology and Prevention; National Heart, Lung, and Blood Institute; American Heart Association; World Heart Federation; International Atherosclerosis Society; and International Association for the Study of Obesity. Circulation 120:1640–1645 doi:10.1161/CIRCULATIONAHA.109.192644 [PubMed: 19805654]
2. Bagno L, Hatzistergos KE, Balkan W, Hare JM (2018) Mesenchymal Stem Cell-Based Therapy for Cardiovascular Disease: Progress and Challenges. Mol Ther 26:1610–1623 doi:10.1016/j.ymthe.2018.05.009 [PubMed: 29807782]
3. Baranyai T, Herczeg K, Onodi Z, Voszka I, Modos K, Marton N, Nagy G, Mager I, Wood MJ, El Andaloussi S, Palinkas Z, Kumar V, Nagy P, Kittel A, Buzas EI, Ferdinandy P, Giricz Z (2015) Isolation of Exosomes from Blood Plasma: Qualitative and Quantitative Comparison of Ultracentrifugation and Size Exclusion Chromatography Methods. PLoS One 10:e0145686 doi:10.1371/journal.pone.0145686 [PubMed: 26690353]
4. Chrysochou C, Kalra PA (2009) Epidemiology and natural history of atherosclerotic renovascular disease. Prog Cardiovasc Dis 52:184–195 doi:10.1016/j.pcad.2009.09.001 [PubMed: 19917329]
5. Davidson SM, Andreadou I, Barile L, Birnbaum Y, Cabrera-Fuentes HA, Cohen MV, Downey JM, Girao H, Pagliaro P, Penna C, Pernow J, Preissner KT, Ferdinandy P (2019) Circulating blood cells and extracellular vesicles in acute cardioprotection. Cardiovasc Res 115:1156–1166 doi:10.1093/cvr/cvy314 [PubMed: 30590395]
6. Davies MG, Saad WE, Bismuth J, Naoum JJ, Peden EK, Lumsden AB (2010) Impact of metabolic syndrome on the outcomes of percutaneous renal angioplasty and stenting. J Vasc Surg 51:926–932 doi:10.1016/j.jvs.2009.09.042 [PubMed: 20022208]
7. Eckel RH, Krauss RM (1998) American Heart Association call to action: obesity as a major risk factor for coronary heart disease. AHA Nutrition Committee. Circulation 97:2099–2100 [PubMed: 9626167]
8. Eirin A, Ebrahimi B, Zhang X, Zhu XY, Tang H, Crane JA, Lerman A, Textor SC, Lerman LO (2012) Changes in glomerular filtration rate after renal revascularization correlate with microvascular hemodynamics and inflammation in Swine renal artery stenosis. Circ Cardiovasc Interv 5:720–728 doi:10.1161/CIRCINTERVENTIONS.112.972596 [PubMed: 23048054]
9. Eirin A, Gloviczki ML, Tang H, Gossl M, Jordan KL, Woollard JR, Lerman A, Grande JP, Textor SC, Lerman LO (2013) Inflammatory and injury signals released from the post-stenotic human kidney. Eur Heart J 34:540–548a doi:10.1093/eurheartj/ehs197 [PubMed: 22771675]

10. Eirin A, Williams BJ, Ebrahimi B, Zhang X, Crane JA, Lerman A, Textor SC, Lerman LO (2014) Mitochondrial targeted peptides attenuate residual myocardial damage after reversal of experimental renovascular hypertension. J Hypertens 32:154–165 doi:10.1097/HJH.0b013e3283658a53 [PubMed: 24048008]
11. Eirin A, Zhang X, Zhu XY, Tang H, Jordan KL, Grande JP, Dietz AB, Lerman A, Textor SC, Lerman LO (2014) Renal vein cytokine release as an index of renal parenchymal inflammation in chronic experimental renal artery stenosis. Nephrol Dial Transplant 29:274–282 doi:10.1093/ndt/gft305 [PubMed: 24097799]
12. Eirin A, Zhu XY, Ebrahimi B, Krier JD, Riester SM, van Wijnen AJ, Lerman A, Lerman LO (2015) Intrarenal Delivery of Mesenchymal Stem Cells and Endothelial Progenitor Cells Attenuates Hypertensive Cardiomyopathy in Experimental Renovascular Hypertension. Cell Transplant 24:2041–2053 doi:10.3727/096368914X685582 [PubMed: 25420012]
13. Eirin A, Zhu XY, Ferguson CM, Riester SM, van Wijnen AJ, Lerman A, Lerman LO (2015) Intrarenal delivery of mesenchymal stem cells attenuates myocardial injury after reversal of hypertension in porcine renovascular disease. Stem Cell Res Ther 6:7 doi:10.1186/scrt541 [PubMed: 25599803]
14. Eirin A, Zhu XY, Jonnada S, Lerman A, van Wijnen AJ, Lerman LO (2018) Mesenchymal Stem Cell-Derived Extracellular Vesicles Improve the Renal Microvasculature in Metabolic Renovascular Disease in Swine. Cell Transplant 27:1080–1095 doi:10.1177/0963689718780942 [PubMed: 29954220]
15. Eirin A, Zhu XY, Krier JD, Tang H, Jordan KL, Grande JP, Lerman A, Textor SC, Lerman LO (2012) Adipose tissue-derived mesenchymal stem cells improve revascularization outcomes to restore renal function in swine atherosclerotic renal artery stenosis. Stem Cells 30:1030–1041 doi:10.1002/stem.1047 [PubMed: 22290832]
16. Eirin A, Zhu XY, Puranik AS, Tang H, McGurren KA, van Wijnen AJ, Lerman A, Lerman LO (2017) Mesenchymal stem cell-derived extracellular vesicles attenuate kidney inflammation. Kidney Int 92:114–124 doi:10.1016/j.kint.2016.12.023 [PubMed: 28242034]
17. Eirin A, Zhu XY, Puranik AS, Woollard JR, Tang H, Dasari S, Lerman A, van Wijnen AJ, Lerman LO (2017) Integrated transcriptomic and proteomic analysis of the molecular cargo of extracellular vesicles derived from porcine adipose tissue-derived mesenchymal stem cells. PLoS One 12:e0174303 doi:10.1371/journal.pone.0174303 [PubMed: 28333993]
18. Gansevoort RT, Correa-Rotter R, Hemmelgarn BR, Jafar TH, Heerspink HJ, Mann JF, Matsushita K, Wen CP (2013) Chronic kidney disease and cardiovascular risk: epidemiology, mechanisms, and prevention. Lancet 382:339–352 doi:10.1016/S0140-6736(13)60595-4 [PubMed: 23727170]
19. Haarer J, Johnson CL, Soeder Y, Dahlke MH (2015) Caveats of mesenchymal stem cell therapy in solid organ transplantation. Transpl Int 28:1–9 doi:10.1111/tri.12415
20. Halberg N, Khan T, Trujillo ME, Wernstedt-Asterholm I, Attie AD, Sherwani S, Wang ZV, Landskroner-Eiger S, Dineen S, Magalang UJ, Brekken RA, Scherer PE (2009) Hypoxia-inducible factor 1alpha induces fibrosis and insulin resistance in white adipose tissue. Mol Cell Biol 29:4467–4483 doi:10.1128/MCB.00192-09 [PubMed: 19546236]
21. Hayer MK, Price AM, Liu B, Baig S, Ferro CJ, Townend JN, Steeds RP, Edwards NC (2018) Diffuse Myocardial Interstitial Fibrosis and Dysfunction in Early Chronic Kidney Disease. Am J Cardiol 121:656–660 doi:10.1016/j.amjcard.2017.11.041 [PubMed: 29366457]
22. He J, Wang Y, Lu X, Zhu B, Pei X, Wu J, Zhao W (2015) Micro-vesicles derived from bone marrow stem cells protect the kidney both in vivo and in vitro by microRNA-dependent repairing. Nephrology (Carlton) 20:591–600 doi:10.1111/nep.12490 [PubMed: 25907000]
23. Higuchi Y, Otsu K, Nishida K, Hirotani S, Nakayama H, Yamaguchi O, Matsumura Y, Ueno H, Tada M, Hori M (2002) Involvement of reactive oxygen species-mediated NF-kappa B activation in TNF-alpha-induced cardiomyocyte hypertrophy. J Mol Cell Cardiol 34:233–240 doi:10.1006/jmcc.2001.1505 [PubMed: 11851362]
24. Jurk D, Wang C, Miwa S, Maddick M, Korolchuk V, Tsolou A, Gonos ES, Thrasivoulou C, Saffrey MJ, Cameron K, von Zglinicki T (2012) Postmitotic neurons develop a p21-dependent senescence-like phenotype driven by a DNA damage response. Aging Cell 11:996–1004 doi:10.1111/j.1474-9726.2012.00870.x [PubMed: 22882466]

25. Katsiki N, Athyros VG, Karagiannis A, Mikhailidis DP (2014) Metabolic syndrome and non-cardiac vascular diseases: an update from human studies. Curr Pharm Des 20:4944–4952 [PubMed: 24320038]
26. Khangura KK, Eirin A, Kane GC, Misra S, Textor SC, Lerman A, Lerman LO (2014) Cardiac function in renovascular hypertensive patients with and without renal dysfunction. Am J Hypertens 27:445–453 doi:10.1093/ajh/hpt203 [PubMed: 24162729]
27. Kingma JG, Simard D, Rouleau JR, Drolet B, Simard C (2017) The Physiopathology of Cardiorenal Syndrome: A Review of the Potential Contributions of Inflammation. J Cardiovasc Dev Dis 4 doi:10.3390/jcdd4040021
28. Kirkland JL, Tchkonia T (2017) Cellular Senescence: A Translational Perspective. EBioMedicine 21:21–28 doi:10.1016/j.ebiom.2017.04.013 [PubMed: 28416161]
29. Kunter U, Rong S, Boor P, Eitner F, Muller-Newen G, Djuric Z, van Roeyen CR, Konieczny A, Ostendorf T, Villa L, Milovanceva-Popovska M, Kerjaschki D, Floege J (2007) Mesenchymal stem cells prevent progressive experimental renal failure but maldifferentiate into glomerular adipocytes. J Am Soc Nephrol 18:1754–1764 doi:10.1681/ASN.2007010044 [PubMed: 17460140]
30. Lawson C, Kovacs D, Finding E, Ulfelder E, Luis-Fuentes V (2017) Extracellular Vesicles: Evolutionarily Conserved Mediators of Intercellular Communication. Yale J Biol Med 90:481–491 [PubMed: 28955186]
31. Lerman LO, Schwartz RS, Grande JP, Sheedy PF, Romero JC (1999) Noninvasive evaluation of a novel swine model of renal artery stenosis. J Am Soc Nephrol 10:1455–1465 [PubMed: 10405201]
32. Lin J, Zhu X, Chade AR, Jordan KL, Lavi R, Daghini E, Gibson ME, Guglielmotti A, Lerman A, Lerman LO (2009) Monocyte chemoattractant proteins mediate myocardial microvascular dysfunction in swine renovascular hypertension. Arterioscler Thromb Vasc Biol 29:1810–1816 doi:10.1161/ATVBAHA.109.190546 [PubMed: 19628782]
33. Machado MV, Vieira AB, da Conceicao FG, Nascimento AR, da Nobrega ACL, Tibirica E (2017) Exercise training dose differentially alters muscle and heart capillary density and metabolic functions in an obese rat with metabolic syndrome. Exp Physiol 102:1716–1728 doi:10.1113/EP086416 [PubMed: 28921743]
34. Malaquin N, Martinez A, Rodier F (2016) Keeping the senescence secretome under control: Molecular reins on the senescence-associated secretory phenotype. Exp Gerontol 82:39–49 doi:10.1016/j.exger.2016.05.010 [PubMed: 27235851]
35. Minamino T, Orimo M, Shimizu I, Kunieda T, Yokoyama M, Ito T, Nojima A, Nabetani A, Oike Y, Matsubara H, Ishikawa F, Komuro I (2009) A crucial role for adipose tissue p53 in the regulation of insulin resistance. Nat Med 15:1082–1087 doi:10.1038/nm.2014 [PubMed: 19718037]
36. Nascimento AR, Machado M, de Jesus N, Gomes F, Lessa MA, Bonomo IT, Tibirica E (2013) Structural and functional microvascular alterations in a rat model of metabolic syndrome induced by a high-fat diet. Obesity (Silver Spring) 21:2046–2054 doi:10.1002/oby.20358 [PubMed: 23512529]
37. Pawar AS, Zhu XY, Eirin A, Tang H, Jordan KL, Woollard JR, Lerman A, Lerman LO (2015) Adipose tissue remodeling in a novel domestic porcine model of diet-induced obesity. Obesity (Silver Spring) 23:399–407 doi:10.1002/oby.20971 [PubMed: 25627626]
38. Reinders ME, Leuning DG, de Fijter JW, Hoogduijn MJ, Rabelink TJ (2014) Mesenchymal stromal cell therapy for cardio renal disorders. Curr Pharm Des 20:2412–2429 [PubMed: 23844816]
39. Ronco C, Di Lullo L (2017) Cardiorenal Syndrome in Western Countries: Epidemiology, Diagnosis and Management Approaches. Kidney Dis (Basel) 2:151–163 doi:10.1159/000448749 [PubMed: 28232932]
40. Saad A, Dietz AB, Herrmann SMS, Hickson LJ, Glockner JF, McKusick MA, Misra S, Bjarnason H, Armstrong AS, Gastineau DA, Lerman LO, Textor SC (2017) Autologous Mesenchymal Stem Cells Increase Cortical Perfusion in Renovascular Disease. J Am Soc Nephrol 28:2777–2785 doi:10.1681/ASN.2017020151 [PubMed: 28461553]
41. Saad A, Herrmann SM, Crane J, Glockner JF, McKusick MA, Misra S, Eirin A, Ebrahimi B, Lerman LO, Textor SC (2013) Stent revascularization restores cortical blood flow and reverses tissue hypoxia in atherosclerotic renal artery stenosis but fails to reverse inflammatory pathways or

glomerular filtration rate. Circ Cardiovasc Interv 6:428–435 doi:10.1161/CIRCINTERVENTIONS.113.000219 [PubMed: 23899868]

42. Sluijter JPG, Davidson SM, Boulanger CM, Buzas EI, de Kleijn DPV, Engel FB, Giricz Z, Hausenloy DJ, Kishore R, Lecour S, Leor J, Madonna R, Perrino C, Prunier F, Sahoo S, Schiffelers RM, Schulz R, Van Laake LW, Ytrehus K, Ferdinandy P (2018) Extracellular vesicles in diagnostics and therapy of the ischaemic heart: Position Paper from the Working Group on Cellular Biology of the Heart of the European Society of Cardiology. Cardiovasc Res 114:19–34 doi:10.1093/cvr/cvx211 [PubMed: 29106545]
43. Smith GL, Masoudi FA, Shlipak MG, Krumholz HM, Parikh CR (2008) Renal impairment predicts long-term mortality risk after acute myocardial infarction. J Am Soc Nephrol 19:141–150 doi:10.1681/ASN.2007050554 [PubMed: 18003773]
44. Sorrentino JA, Sanoff HK, Sharpless NE (2014) Defining the toxicology of aging. Trends Mol Med 20:375–384 doi:10.1016/j.molmed.2014.04.004 [PubMed: 24880613]
45. Stenvinkel P, Luttropp K, McGuinness D, Witasp A, Qureshi AR, Wernerson A, Nordfors L, Schalling M, Ripsweden J, Wennberg L, Soderberg M, Barany P, Olauson H, Shiels PG (2017) CDKN2A/p16INK4(a) expression is associated with vascular progeria in chronic kidney disease. Aging (Albany NY) 9:494–507 doi:10.18632/aging.101173 [PubMed: 28192277]
46. Sun R, Zhu B, Xiong K, Sun Y, Shi D, Chen L, Zhang Y, Li Z, Xue L (2017) Senescence as a novel mechanism involved in beta-adrenergic receptor mediated cardiac hypertrophy. PLoS One 12:e0182668 doi:10.1371/journal.pone.0182668 [PubMed: 28783759]
47. Suthahar N, Meijers WC, Sillje HHW, de Boer RA (2017) From Inflammation to Fibrosis-Molecular and Cellular Mechanisms of Myocardial Tissue Remodelling and Perspectives on Differential Treatment Opportunities. Curr Heart Fail Rep 14:235–250 doi:10.1007/s11897-017-0343-y [PubMed: 28707261]
48. Thomas G, Sehgal AR, Kashyap SR, Srinivas TR, Kirwan JP, Navaneethan SD (2011) Metabolic syndrome and kidney disease: a systematic review and meta-analysis. Clin J Am Soc Nephrol 6:2364–2373 doi:10.2215/CJN.02180311 [PubMed: 21852664]
49. Uchida Y, Ichimiya S, Ishii H, Kanashiro M, Watanabe J, Yoshikawa D, Takeshita K, Sakai S, Amano T, Matsubara T, Murohara T (2012) Impact of metabolic syndrome on various aspects of microcirculation and major adverse cardiac events in patients with ST-segment elevation myocardial infarction. Circ J 76:1972–1979 [PubMed: 22664935]
50. Urbieta-Caceres VH, Zhu XY, Jordan KL, Tang H, Textor K, Lerman A, Lerman LO (2012) Selective improvement in renal function preserved remote myocardial microvascular integrity and architecture in experimental renovascular disease. Atherosclerosis 221:350–358 doi:10.1016/j.atherosclerosis.2011.10.005 [PubMed: 22341593]
51. Wali RK, Wang GS, Gottlieb SS, Bellumkonda L, Hansalia R, Ramos E, Drachenberg C, Papadimitriou J, Brisco MA, Blahut S, Fink JC, Fisher ML, Bartlett ST, Weir MR (2005) Effect of kidney transplantation on left ventricular systolic dysfunction and congestive heart failure in patients with end-stage renal disease. J Am Coll Cardiol 45:1051–1060 doi:10.1016/j.jacc.2004.11.061 [PubMed: 15808763]
52. Welnicki MT, Sliz DI, Szeligowska J, Duda-Krol WB, Chomiuk T, Dabrowska D, Drozdz J, Mamcarz AJ (2018) The influence of metabolic syndrome coexistence on the prognosis of patients with heart failure without atrial fibrillation. Analysis of Polish data from the pilot survey for the ESC Heart Failure Registry. Kardiol Pol 76:794–796 doi:10.5603/KP.2018.0077 [PubMed: 29652423]
53. Yuan F, Hedayat AF, Ferguson CM, Lerman A, Lerman LO, Eirin A (2018) Mitoprotection attenuates myocardial vascular impairment in porcine metabolic syndrome. Am J Physiol Heart Circ Physiol 314:H669–H680 doi:10.1152/ajpheart.00431.2017 [PubMed: 29196345]
54. Zhao L, Cheng G, Jin R, Afzal MR, Samanta A, Xuan YT, Girgis M, Elias HK, Zhu Y, Davani A, Yang Y, Chen X, Ye S, Wang OL, Chen L, Hauptman J, Vincent RJ, Dawn B (2016) Deletion of Interleukin-6 Attenuates Pressure Overload-Induced Left Ventricular Hypertrophy and Dysfunction. Circ Res 118:1918–1929 doi:10.1161/CIRCRESAHA.116.308688 [PubMed: 27126808]

55. Zhu XY, Daghini E, Chade AR, Napoli C, Ritman EL, Lerman A, Lerman LO (2007) Simvastatin prevents coronary microvascular remodeling in renovascular hypertensive pigs. J Am Soc Nephrol 18:1209–1217 doi:10.1681/ASN.2006090976 [PubMed: 17344424]

56. Zhu XY, Ebrahimi B, Eirin A, Woollard JR, Tang H, Jordan KL, Ofori M, Saad A, Herrmann SM, Dietz AB, Textor SC, Lerman A, Lerman LO (2015) Renal Vein Levels of MicroRNA-26a Are Lower in the Poststenotic Kidney. J Am Soc Nephrol 26:1378–1388 doi:10.1681/ASN.2014030248 [PubMed: 25270070]

57. Zhu XY, Urbieta-Caceres V, Krier JD, Textor SC, Lerman A, Lerman LO (2013) Mesenchymal stem cells and endothelial progenitor cells decrease renal injury in experimental swine renal artery stenosis through different mechanisms. Stem Cells 31:117–125 doi:10.1002/stem.1263 [PubMed: 23097349]

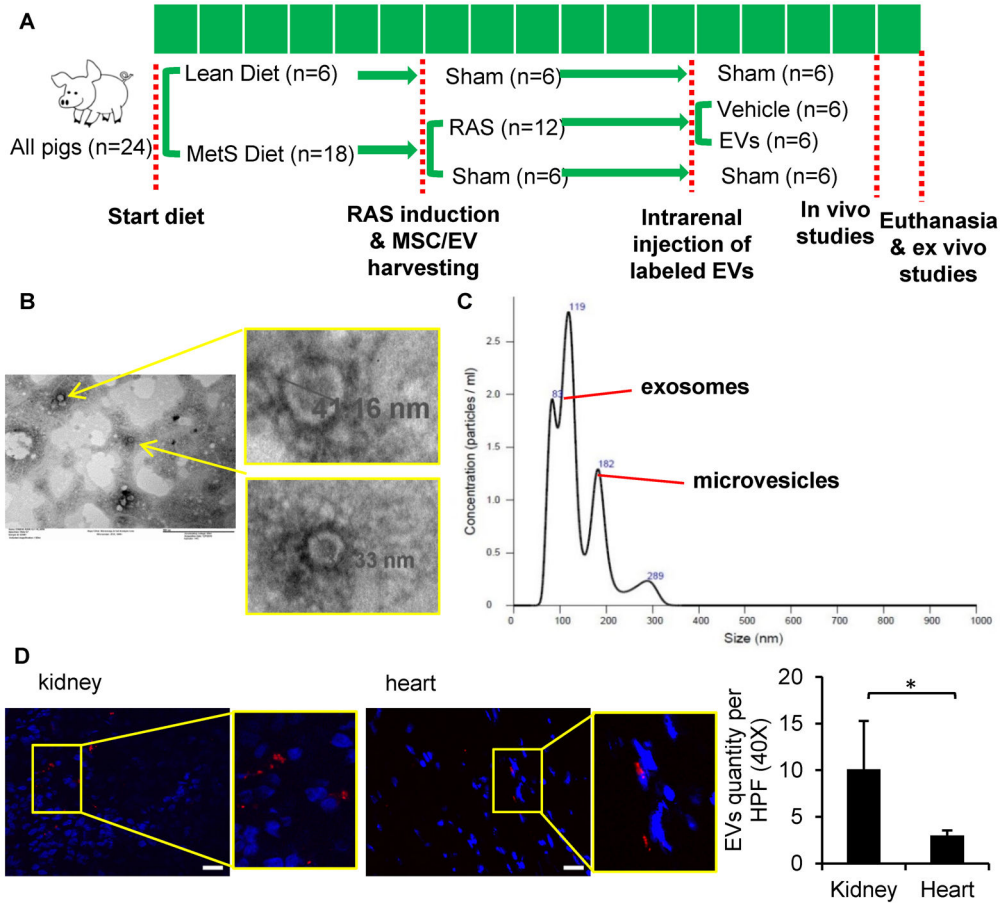

Figure 1.

Characterization and tracking of swine mesenchymal stromal/stem cell (MSC)-derived extracellular vesicles (EVs). (A) Schematic of the experimental protocol. (B) Transmission electron microscopy images of EVs. (C) NanoSight analysis showing size distribution of EVs as exosomes and microvesicles. (D) Threefold-greater numbers of PKH-26-labeled EVs were detected in frozen sections from the stenotic kidney compared to the heart. *p<0.05. Scale bar =50μm.

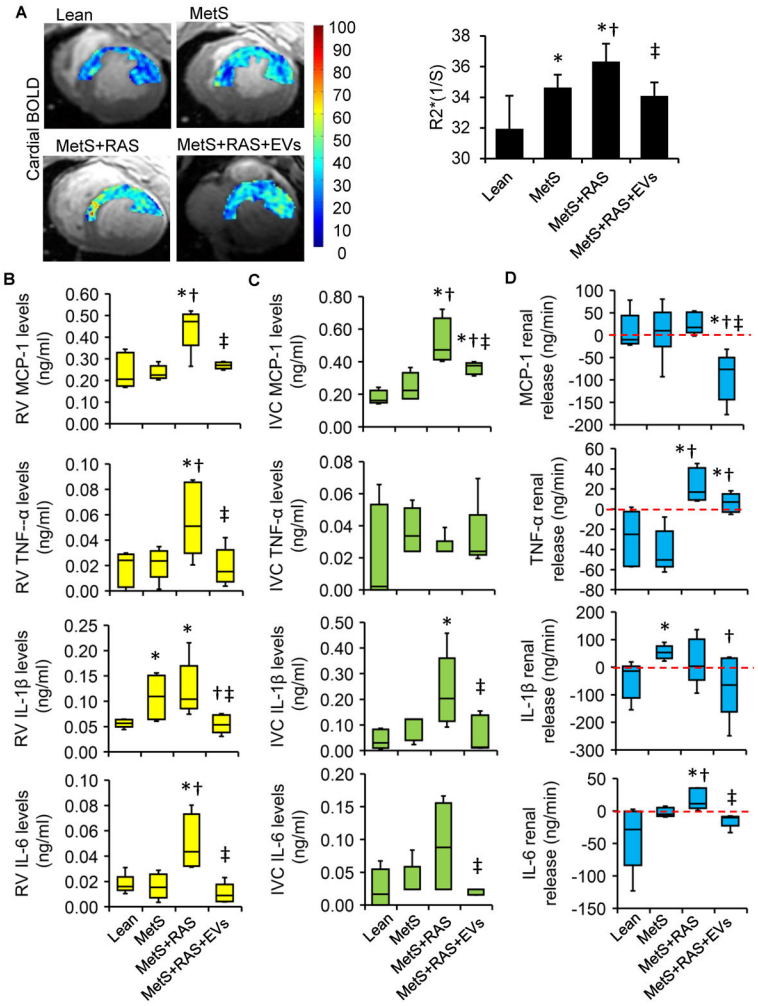

Figure 2.

Extracellular vesicles (EVs) improved myocardial oxygenation and microcirculation, and reduced renal and systemic inflammation. (A) Representative blood oxygen-level-dependent (BOLD) magnetic resonance images of the left ventricular (LV) and quantification of R2* index. Levels of monocyte-chemoattractant protein (MCP)-1, tumor necrosis-factor (TNF)-α, interleukin (IL)-6, and IL-1ß in Lean, MetS, MetS+RAS, MetS+RAS+EVs and MetS +EVs in renal vein (RV) (B) and the systemic circulation (C). (D) Respective net release by the stenotic kidney. n=5-6/group. *p<0.05 vs. Lean, †p<0.05 vs. MetS, ‡p<0.05 vs. MetS +RAS.

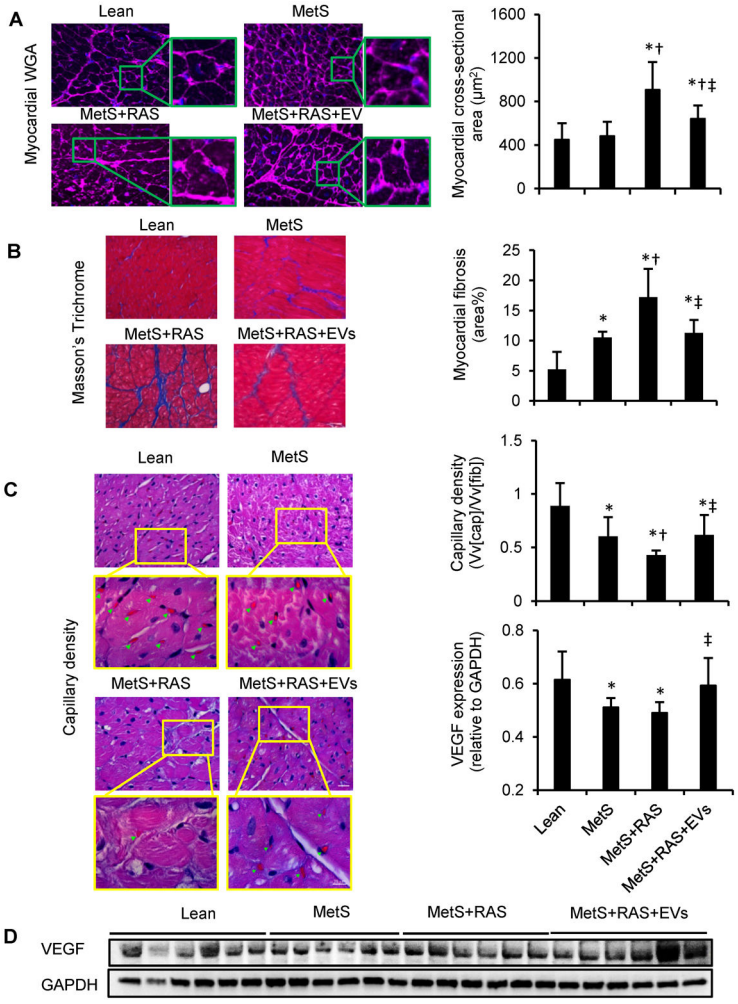

Figure 3.

Extracellular vesicles (EVs) alleviated myocardial remodeling and fibrosis. (A) Left-ventricular sections stained with wheat germ agglutinin (WGA) and quantification of myocyte cross-sectional area. (B) Representative staining and quantification of Masson's Trichrome. n=6/group. (C) Representative LV sections stained with hematoxylin and eosin, showing capillaries (green arrowheads) and density quantification. (D) Western blotting of vascular endothelial growth-factor (VEGF) in LV. n=6/group. *p<0.05 vs. Lean, †p<0.05 vs. MetS, ‡p<0.05 vs. MetS+RAS. Scale bar=50μm.

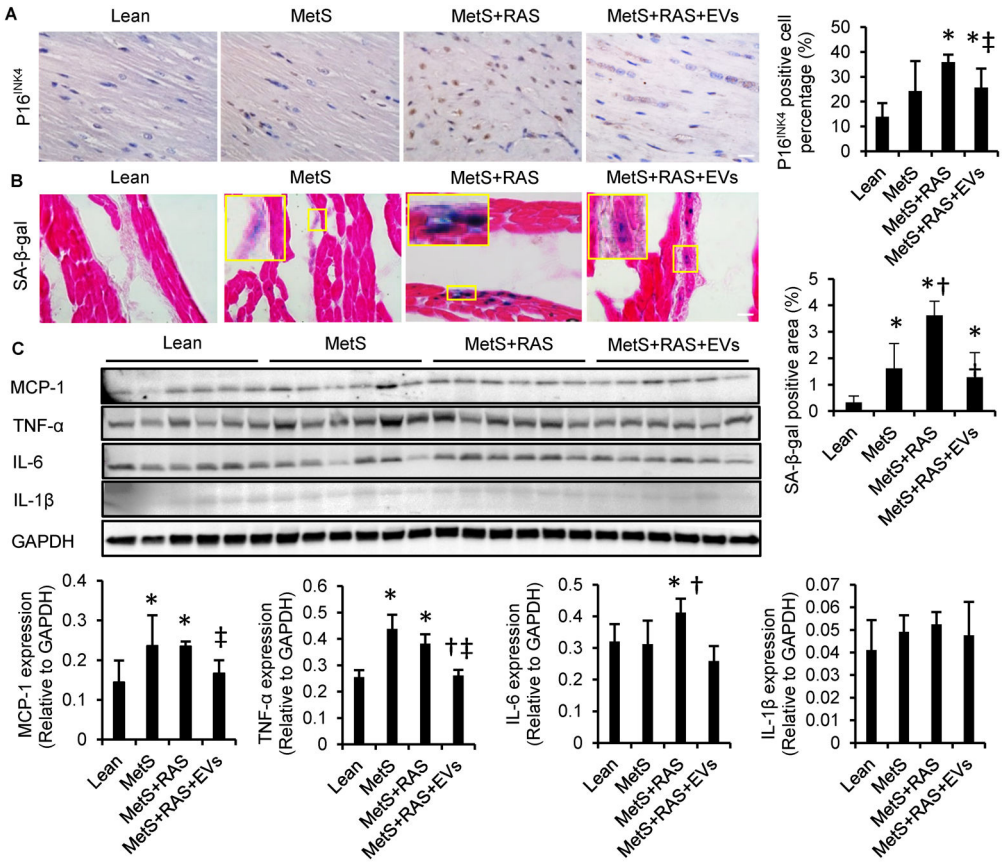

Figure 4.

Extracellular vesicles (EVs) ameliorated myocardial cellular senescence-like phenotype and attenuated myocardial inflammation. (A) Representative immunohistochemical left-ventricular (LV) staining with $p16^{INK4}$ and quantification. (B) LV sections stained with senescence-associated beta-galactosidase (SA-ß-gal, [blue]) and eosin (red) at pH 6, and quantification. n=6/group. (C) Western blotting of LV monocyte-chemoattractant protein (MCP)-1, tumor necrosis-factor (TNF)-a, interleukin (IL)-6, and IL-1ß and quantification. n=6/group. *p<0.05 vs. Lean, †p<0.05 vs. MetS, ‡p<0.05 vs. MetS+RAS. Scale bar=50μm.

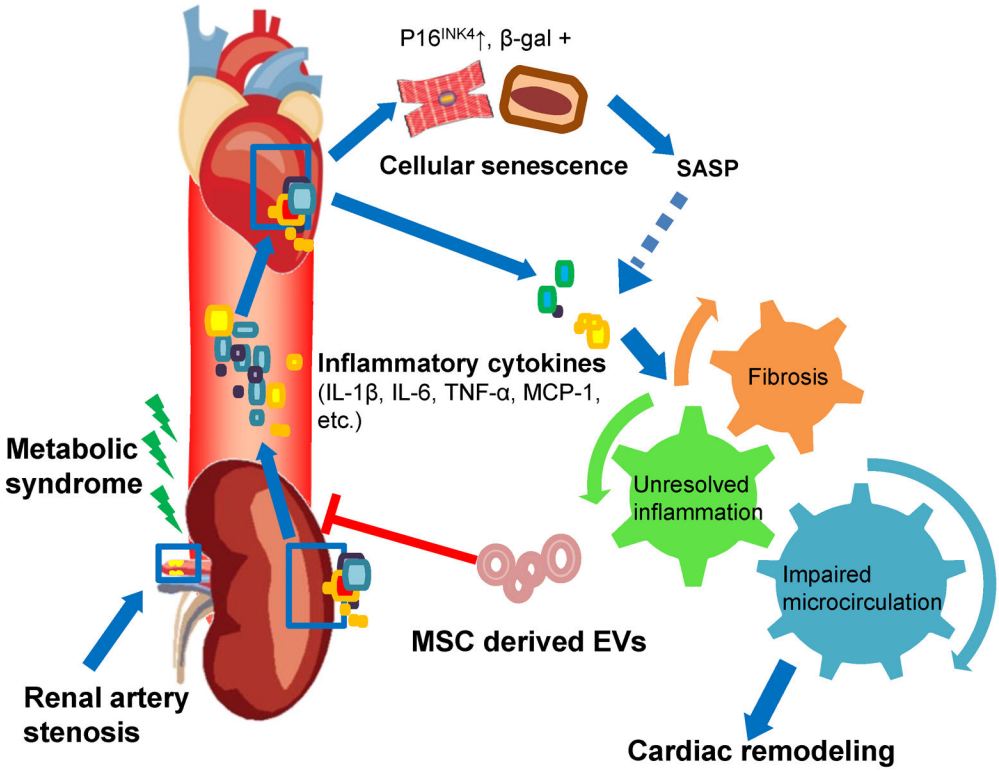

Figure 5.

Schematic illustrating proposed mechanisms by which intrarenal extracellular vesicles attenuate remote myocardial injury in experimental metabolic renovascular disease.

Table 1.

Systemic characteristics, single renal and cardiac function in study groups at 16 weeks

Parameter	Lean n=6	MetS n=6	MetS+RAS n=6	MetS+RAS+EVs n=6	MetS+EVs n=4
Weight (kg)	61.83±3.25	81.67±6.12 *	86.17±9.00 *	88.83±5.27 *	*85.67±3.79* *
MAP (mmHg)	97.33±9.82	101.17±8.18	116.44±14.48 *†	118.94±8.20 *†	*116.89±6.17* *†
Degree of stenosis (%)	0	0	77.50±12.14 *†	70.00±12.65 *†	*0*
Serum creatinine (mg/dl)	1.57±0.34	1.86±0.30	1.94±0.05 *	1.73±0.20‡	*1.88*±0.23
Heart rate (bpm)	82.33±17.13	76.17±16.46	91.17±18.35	77.83±17.94	*72.67±23.50*
EDV(ml)	114.59±26.61	130.72±26.01	135.80±24.23	141.28±14.83	*142.39±20.37*
ESV(ml)	56.57±14.91	66.23±11.86	61.64±14.53	65.68±9.04	*65.37±13.06*
Stroke volume (ml)	58.02±13.85	64.48±15.44	74.16±14.18	75.59±7.41 *	*77.02±7.42*
Ejection fraction (%)	50.85±5.89	49.05±3.66	54.72±5.70	53.60±2.97	*54.36±2.92*
Cardiac output(L/min)	4.76±1.47	4.87±1.60	6.56±0.71 *†	5.80±1.02	*5.48±1.28*
Cardiac index(L/min/kg)	0.08±0.02	0.06±0.02	0.08±0.01†	0.07±0.01 *	*0.06±0.01*
SVR (mmHg.min.ml^{-1})	1.76±0.52	1.77±0.44	1.44±0.27	1.68±0.31	*1.77±0.41*
LVMM(g)	123.59±19.31	142.49±14.72	171.99±14.46 *†	149.12±17.09 *‡	*135.01±10.75*‡
E/A ratio	1.23±0.27	1.25±0.30	0.76±0.33 *†	1.14±0.17‡	*1.21±0.16*
Myocardial perfusion(ml/min/g)					
Baseline	0.85±0.19	0.73±0.17	0.79±0.15	0.86±0.17	*0.84±0.17*
Response to adenosine (Δ%)	62.15±35.05	16.78±13.84 *	17.01±3.56 *	38.93±8.40†‡	*34.90±8.21*‡
RBF (ml/min)	526.44±38.72	829.67±169.91 *	538.22±127.64†	922.88±253.00 *‡	*724.41±337.11*
GFR (ml/min)	72.75±13.91	126.31±27.85 *	83.40±9.55†	135.49±33.99 *‡	*101.46±33.98*

E/A, early and late left ventricular filling; EDV, end diastolic volume; ESV, end systolic volume; EVs, extracellular vesicles; GFR, glomerular filtration rate; HR, heart rate; LVMM, left ventricular muscle mass; MAP, mean arterial pressure; MetS, metabolic syndrome; RAS, renal artery stenosis; RBF, renal blood flow; SVR, systemic vascular resistance;

* p <0.05 versus Lean

† p <0.05 versus MetS

‡ p <0.05 versus MetS+RAS.